Automatic Matrix-Based Analysis Method for Extraction of Optical Fiber Parameters from Polarimetric Optical Time Domain Reflectometry Data

J. G. Ellison and A. S. Siddiqui

***Abstract*—Interpretation of polarimetric optical time domain reflectometry (POTDR) data can be time consuming due to the complicated dependence of the state of polarization evolution on the optical fiber parameters. In this paper, a fully automatic matrix-based analysis method is presented which can extract the linear birefringence and external twist rate from relative backscattered state of polarization data, without error propagation. Practical measurements on fiber samples demonstrate the capability of the technique.**

***Index Terms*—Optical fiber characterization, optical fiber measurements, optical fiber polarization, optical time domain reflectometry (OTDR), polarimetry.**

I. Introduction

RECENTLY, it has been shown [1], [2] how the single-ended technique of polarimetric optical time domain reflectometry (POTDR [3], [4]) can spatially resolve the magnitude of the linear birefringence and external twist rate along an optical fiber. These parameters are important since they determine the local differential group delay (DGD) and hence the end to end polarization mode dispersion (PMD) of an optical fiber link [5], [6]. The analysis method used in [1], [2] extracted the fiber parameters by performing a best fit between the measured backscattered state of polarization (SOP) evolution and the calculated SOP evolution based on a given linear birefringence and twist rate. Such a scheme gives accurate results but places a high reliance on operator ability in selection of the best input SOP and determination of the optimum parameters for the best fit.

A possible operator independent method of extracting the fiber parameters has been suggested in [7] where a backscatter matrix for each fiber element is calculated by measuring the backscattered SOP for a number of different input SOPs. From the backscatter matrices it is possible to determine the transfer function of each fiber element in terms of the parameters of a general elliptical retarder (GER). One of the problems with this technique is relating the parameters of the GER for each fiber element to the internal linear birefringence and external twist rate, since it is the latter parameters that more directly allow the DGD to be determined. Two further drawbacks are the propagation of errors along the fiber and the necessity of measuring the absolute SOP of the backscattered light with respect to the laboratory reference frame.

In this paper an analysis technique is presented which directly gives the spatial evolution of the internal linear birefringence and twist rate from a measurement of three consecutive backscatter matrices. The method has the advantage of only requiring the relative backscattered SOP to be measured, i.e., any rotation of the backscattered SOP evolution on the Poincaré sphere due to connecting fiber between the POTDR instrument and the fiber under test becomes irrelevant. This fact is important since it considerably eases the design of the POTDR and makes the technique directly applicable to the POTDR instrument described in [1]. Furthermore, the problem of error propagation mentioned in [7] is eliminated with this technique.

II. Theory

Fig. 1 shows a schematic representation of the front end of a POTDR. Pulses of known SOP $\vec{S}_{\text{in}}$ are launched into the fiber via a 3 dB coupler. Rayleigh backscattering occurs continuously as the pulse travels along the fiber, resulting in a time-varying output SOP $\vec{S}_{\text{out}}$.

Assuming that the fiber section depicted exhibits uniform linear birefringence and twist then, at a given point l in the fiber, the total transfer Mueller matrix describing the forward-return path is given by

$$\vec{S}_{\text{out}} = \mathbf{R}_{\text{return}}(x_2, y_2, z_2)\mathbf{R}_{\text{fiber}}(\tau, \beta_L, l) \cdot \mathbf{R}_{\text{forward}}(x_1, y_1, z_1)\vec{S}_{\text{in}} \quad (1)$$

where $\mathbf{R}_{\text{return}}$ is a rotation matrix describing the arbitrary rotation of the return path and $\mathbf{R}_{\text{forward}}$ is a rotation matrix describing the arbitrary rotation of the forward path. The fiber element under analysis is represented by $\mathbf{R}_{\text{fiber}}$, which describes the rotation matrix of the forward-return path for the element length l in terms of the fundamental fiber parameters: twist rate τ and linear birefringence β_L. It is assumed that any **internal** spin is negligible (i.e., we are not dealing with spun fiber). In [1], [2] it was shown that the forward-return rotation matrix $\mathbf{R}_{\text{fiber}}$ is a linear retarder, given by

$$\mathbf{R}_{\text{fiber}} = \mathbf{R}^T(\vec{\beta}_F, l)\mathbf{R}_M\mathbf{R}(\vec{\beta}_F, l) \quad (2)$$

Manuscript received February 2, 2000; revised May 22, 2000. This work was carried out under EPSRC (UK) research Grant GR/L/62832. The industrial partners are BT Laboratories and Alcatel Submarine Networks.

The authors are with the Electronic Systems Engineering Department of the University of Essex, Wivenhoe Park, Colchester CO4 3SQ, U.K.

Publisher Item Identifier S 0733-8724(00)08068-3.

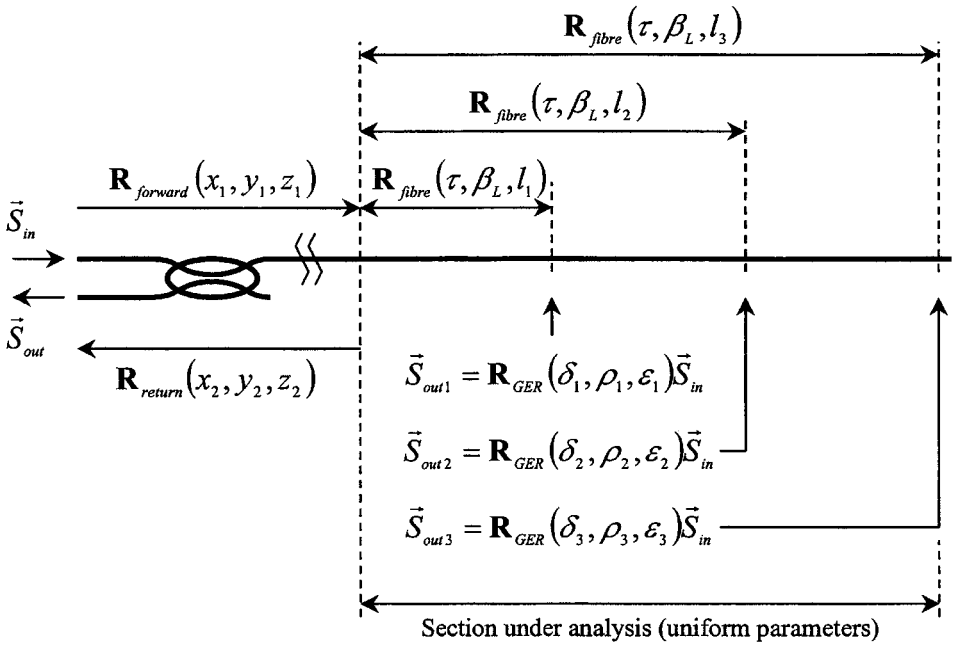

Fig. 1. Transfer Mueller matrices involved in the fiber analysis.

where $\mathbf{R}_M$ is a mirror matrix representing the reflection due to Rayleigh backscattering and $\mathbf{R}(\vec{\beta}_F, l)$ is the forward rotation matrix describing a rotation around the vector $\vec{\beta}_F$ of magnitude $|\vec{\beta}_F|l$. On the Poincaré sphere, the vector $\vec{\beta}_F$ represents the local birefringence vector viewed in a reference frame that rotates with the fiber axes (see Fig. 2), and is given by

$$\vec{\beta}_F = \begin{bmatrix} \beta_L \\ 0 \\ g\tau - 2\tau \end{bmatrix} \tag{3}$$

where g is the stress-optic coefficient. Ideally, one would measure the retardance and orientation of the equivalent linear retarder element $\mathbf{R}_{\text{fiber}}$ and somehow extract the twist rate and linear birefringence from the matrix elements. However, the situation is complicated by the forward and return rotation matrices which "hide" the linear retarder, so that the total transfer matrix up to a point l in the fiber is actually a general elliptical retarder

$$\vec{S}_{\text{out}} = \mathbf{R}_{\text{GER}}(\delta, \rho, \varepsilon)\vec{S}_{\text{in}} \tag{4}$$

where δ is the total retardance, ρ is the azimuth angle of the elliptical retarder and ε is the ellipticity.

It is possible to extract these three defining parameters of $\mathbf{R}_{\text{GER}}$ by launching a minimum of three input SOPs and measuring the corresponding output SOPs. However, there is insufficient information to determine τ and β_L from this measurement since (1) contains eight unknowns (x_1, y_1, z_1, x_2, y_2, z_2, τ and β_L) while (4) only contains three known (δ, ρ and ε). The problem may be solved by repeating the measurement at points further along the fiber to obtain further GERs with different defining parameters (Fig. 1). If it is assumed that the fiber is uniform over the length under analysis, then it is only necessary to measure three consecutive points along the fiber, since this produces nine knowns ($3 \times \delta$, ρ and ε) which exceeds the number of unknowns and allows the twist and linear birefringence to be uniquely determined. Of course, for this method to work accurately the fiber must be uniform over the length of three elements, which implies that the fiber parameters do not change significantly over a distance three times the resolution of the POTDR.

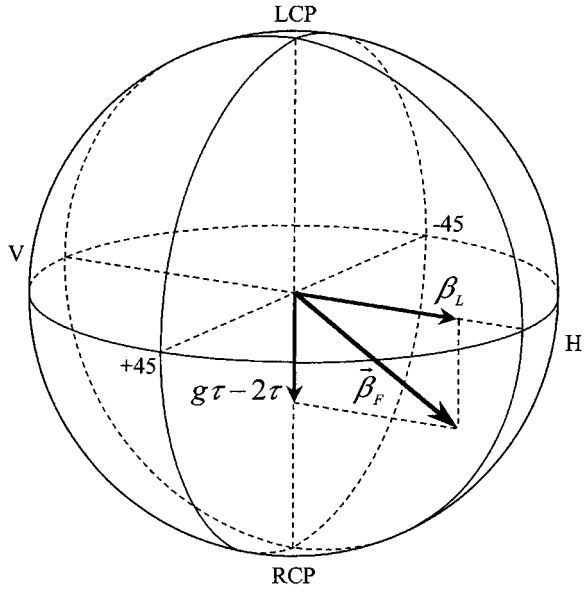

Fig. 2. Birefringence vectors in the rotating reference frame.

The strength of this technique is that it is not necessary to calculate the forward propagating SOP after each analyzing element since all the fiber up to the particular three-element section under analysis can be included in the arbitrary forward and return rotation matrices. Thus fiber at any distance along the fiber can be analyzed without error propagation.

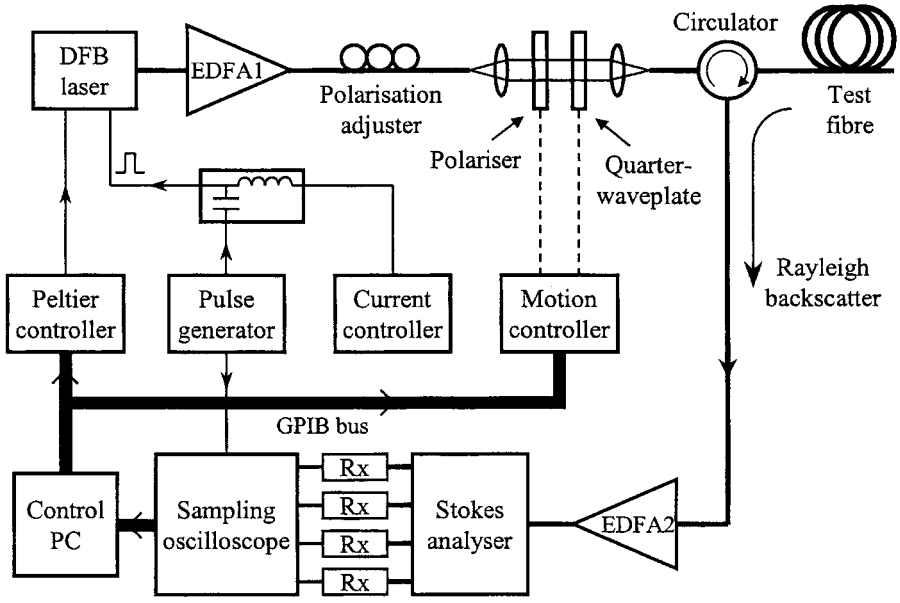

Fig. 3. Schematic layout of POTDR.

To implement the technique effectively using a computer algorithm, a numerical approach was adopted. Based on the POTDR measurement data, the nine matrix elements for $\mathbf{R}_{\mathrm{GER}}$ from each analysis element were obtained, making a total of 27 matrix elements in all. There is some redundancy in the matrix elements due to the symmetry of the rotation matrix for a GER, but this is not important, and in fact provides some indication of the measurement error. Next, seed values of the unknowns $x_1, y_1, z_1, x_2, y_2, z_2, \tau$ and β_L were used to generate three trial GERs based on (1), producing another 27 trial matrix elements. A quasi-Newton method was used to modify the seed values until the 27 trial matrix elements matched the 27 measured matrix elements to within the desired tolerance. The linear birefringence and twist values thus obtained were recorded, and the process repeated for the next analysis section.

III. Experimental Layout

Fig. 3 shows the schematic layout of the POTDR used to take the measurements. High peak power pulses (26 dBm, <10 ns) of known sets of SOPs are generated by the distributed feedback laser diode (DFB), erbium-doped fiber amplifier (EDFA) and quarter-waveplate—polarizer combination and launched into the test fiber via a polarization transparent circulator. The returning Rayleigh backscatter is coupled by the circulator into a low noise 980 nm pumped EDFA and split into the four Stokes components by the bulk optics Stokes Analyzer. The received light is detected by four high sensitivity (16 V/mW), 1.5 GHz bandwidth custom built receivers and fed to a four-channel digitizing oscilloscope that time resolves and averages the four Stokes components prior to transfer to a PC where the SOP and backscatter matrices are calculated and displayed as functions of length. During the averaging process the pulse laser is wavelength dithered by adjustment of its temperature in order to reduce the coherent "speckle" in the backscatter trace caused by the large coherence length of the DFB and the high receiver bandwidth. The probe wavelength is 1550 nm and the pulsewidth is between 3 and 10 ns.

IV. Results

Two samples of unspun dispersion shifted fiber were analyzed with the POTDR. The first 140-m-long sample (fiber 1) was laid out in an oval track roughly 30 m in circumference in order to approximately simulate the conditions of deployment while the second 900 meter long sample (fiber 2) was retained on the shipping bobbin. For fiber 1 the probe pulsewidth was 3 ns giving a spatial resolution of 0.3 m while for fiber 2 the pulsewidth was 10 ns giving a spatial resolution of 1 m.

A. Fiber 1

The backscatter SOP evolution for fiber 1 was recorded for 12 different input SOPs and a least-squares algorithm was used to determine the corresponding backscatter matrix, $\mathbf{R}_{\mathrm{GER}}(l)$, at 0.5-m intervals along the fiber

$$\vec{S}_{\mathrm{out},\,i}(l) = \mathbf{R}_{\mathrm{GER}}(l)\vec{S}_{\mathrm{in},\,i} \tag{5}$$

where i represents the SOP number.

With a 1.5-m step size between analysis elements (i.e., every third backscatter matrix was used) the linear birefringence and twist rate evolution shown in Fig. 4 was obtained. These traces show a number of interesting features. The first of these is the regular appearance roughly every 30 m of a maximum in the twist rate. This corresponds with the loop length and suggests that some systematic twist resulted from the method used to lay out the fiber. It should be noted that the matrix method as it stands does not distinguish well between clockwise and anti-clockwise twist, since in (1) it is possible to generate two rotation matrices, $\mathbf{R}_{\mathrm{return}}$, which result in the same output SOP for opposite values of twist rate. For this reason only the absolute value of twist has been plotted in Fig. 4, although it seems

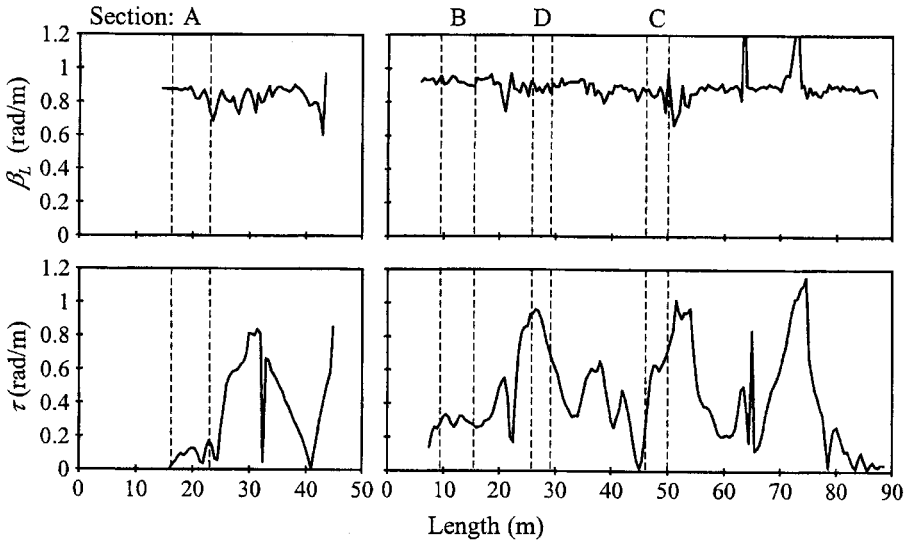

Fig. 4. Linear birefringence and twist rate evolution along two segments of fiber 1 calculated using the matrix method. Highlighted sections have also been analyzed with the best-fit method, shown in Fig. 5.

likely that where the twist reaches zero (e.g., 41 m into the first segment and 45 m into the second segment) the twist rate smoothly changes from one direction to the other rather than the abrupt change depicted in the trace. If direction is important, such as in DGD prediction, ensuring that the rotation matrix elements do not suffer any abrupt changes in value around the zero twist position should allow the transition from one direction to the other to be followed without error.

A second feature in the traces is the appearance of some obviously erroneous values of twist and linear birefringence. At 32 m into the first segment the twist rate undergoes a very abrupt change from a relatively high value to zero and back again. Similar abrupt changes in the linear birefringence occur at 65 and 73 m into the second segment. These errors correspond to positions along the fiber where the Newton method failed to converge and the program loop eventually terminated. The explanation for this behavior lies in the nonuniformity of the twist rate, since the matrix method assumes a uniform linear birefringence and twist rate over the section being analyzed. As can be seen, the large errors occurred where the twist rate was changing rapidly. Similar errors, although not quite as severe, can be seen at other points where a sudden change in twist rate occurs, for instance, at 22 and 51 m into the second segment of fiber. Here, the Newton method did converge, but the calculated values of linear birefringence and twist show a significant deviation from the expected values. Fortunately, such errors are easily identified by either a failure of the algorithm to converge or a high error residual, allowing the points to be removed and possibly replaced with values interpolated from those either side of the suspect measurement point.

As verification of the efficacy of the matrix method, it is useful to compare the computed values of linear birefringence and twist with those obtained using the best fit method detailed in [1], [2]. Fig. 5 shows the measured and best-fit backscattered SOP evolutions for the sections highlighted in Fig. 4, where the input SOP has been chosen to give good symmetry in the generated figure of eight shape. For sections A, B, and C the matrix method gives twist rate values of 0.13 rad/m, 0.31 rad/m and 0.6 rad/m, which compares well with the best-fit values of 0.12 rad/m, 0.34 rad/m and 0.6 rad/m. For section D, the agreement is not quite as good, with the matrix method giving a twist rate of 0.9 rad/m compared to the best-fit value of 1.1 rad/m. This is not unexpected, since the best-fit method begins to show limitations under conditions of high twist rate. The twist rate is also changing quite significantly over the analysis length for this last case, hence the matrix method will tend to produce an average value which is influenced by the reduced twist rate either side of the maximum.

B. Fiber 2

For fiber spooled on a bobbin, the externally induced bending birefringence can reach or exceed the magnitude of the internal linear birefringence. The total linear birefringence vector then becomes the vectorial sum of the stationary externally induced linear birefringence and the rotating internally produced linear birefringence. A maximum in the total linear birefringence occurs when the two vectors coincide and a minimum when they are opposite. Both the best-fit method and the matrix method can be used in unmodified form to extract the local value of the total linear birefringence, provided that the twist rate is sufficiently low to ensure that the internal linear birefringence vector does not rotate significantly over the measurement length. This is equivalent to assuming that $\tau = 0$ in equation (4) and that β_L is the vectorial sum of the externally induced linear birefringence and the (assumed stationary) internally produced linear birefringence. For the worst case of equal internal and external linear birefringence values, the modulation depth is greatest, with the total birefringence value ranging between zero and maximum for every 90° of fiber axis rotation. However, a simple vector calculation shows that if the fiber rotation is less than 18° over the analysis length then the error will be less than 10% of the maximum

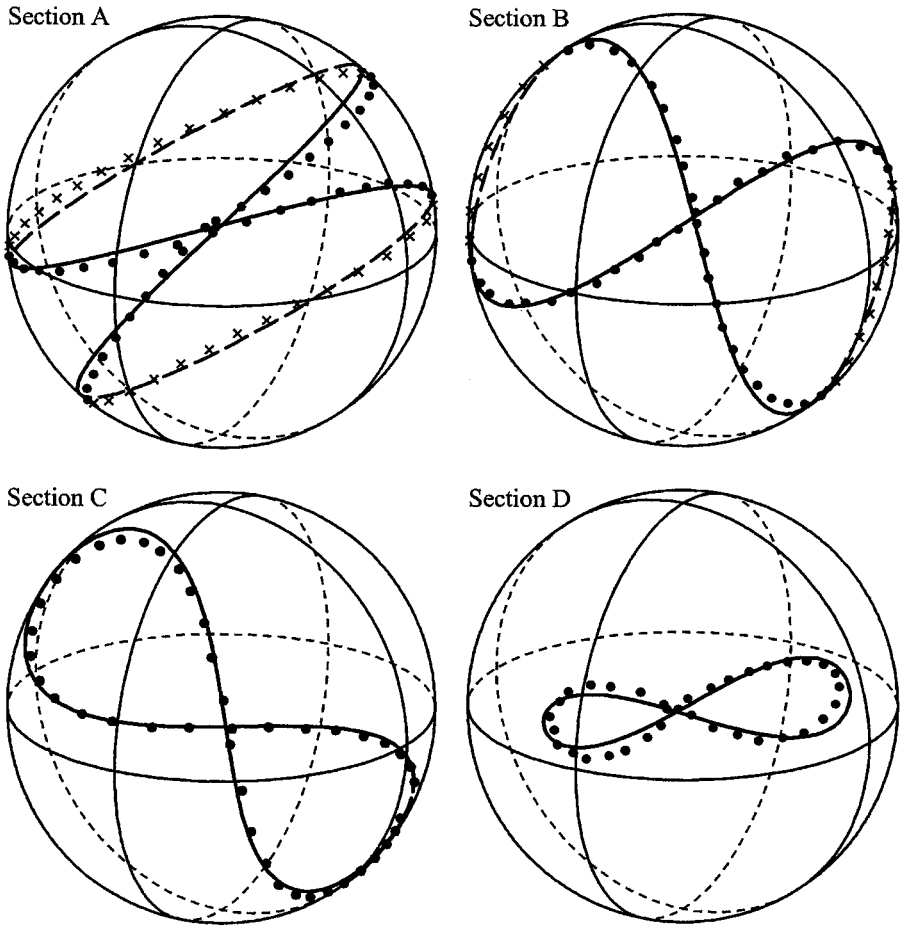

Fig. 5. Measured (points) and best-fit (solid line) backscattered SOP evolution for sections of fiber 1. The linear birefringence is $\beta_L = 0.88$ rad/m for all sections and the twist rates are (Section A) $\tau = 0.12$ rad/m, (Section B) $\tau = 0.34$ rad/m, (Section C) $\tau = 0.6$ rad/m and (Section D) $\tau = 1.1$ rad/m.

value of total birefringence. Extraction of the twist rate itself is more difficult, but one crude method may be to measure the distance between successive maxima in the measured value of total linear birefringence, since these occur every half fiber turn. However, this gives a poor twist rate resolution. Ideally, the method of analysis requires a modification to include the complete vector description. Due to the number of variables this entails, this modification has not been performed, hence for fiber on a bobbin only the linear birefringence can be reliably extracted.

Fig. 6(a) shows the extracted linear birefringence using the matrix method for 900 m of fiber 2 on a 16 cm diameter shipping bobbin. The outer layers of the fiber correspond to smaller length values and vice versa. In contrast to the steady linear birefringence exhibited by fiber 1 in the loop, the linear birefringence for fiber 2 varies quite significantly along the fiber length, this variation becoming more pronounced for the inner layers of fiber. The main cause of the fluctuation is the changing magnitude of the local linear birefringence vector as the rotating internal linear birefringence vector alternately adds to and subtracts from the bending birefringence vector. However, a further error is introduced due to the nonuniformity of the total linear birefringence over the analysis length, which for these measurements was 6 m. The large spikes in the trace, such as at 580 m, are probably a result of this form of error, as well as the points in the fiber where the Newton method failed to converge. These latter points have been excluded for clarity, but their positions can be seen by the missing parts of the trace.

In order to better distinguish the true variation due to the total linear birefringence variation and the false variation due to error, the 900-m length was also analyzed section by section using the best-fit method. The fiber was traversed in roughly 15 m steps, with a uniform section at each step being chosen for analysis. Over 50 of these sections were analyzed by hand in order to build up a picture of the linear birefringence evolution along the fiber. Fig. 6(b) shows the result. Although the magnitude of the variation has been tempered somewhat, the main features of the trace remain, with prominent peaks and troughs occurring in the same places in both Fig. 6(a) and (b). Incidentally, since each section takes around 5–10 min to analyze by hand, the best fit method required almost a whole working day to obtain the results for the 900 m length, compared with around 10 min for the matrix method. Note that the times quoted are purely for analyzing the data and do not include the data gathering itself, which may be anything from five minutes to over an hour, depending on the number of input SOPs chosen, the length of the fiber and the averaging required.

One interesting feature which is visible in both the matrix analysis [Fig. 6(a)] and the best-fit analysis [Fig. 6(b)] is the presence of steps in the linear birefringence value near to the

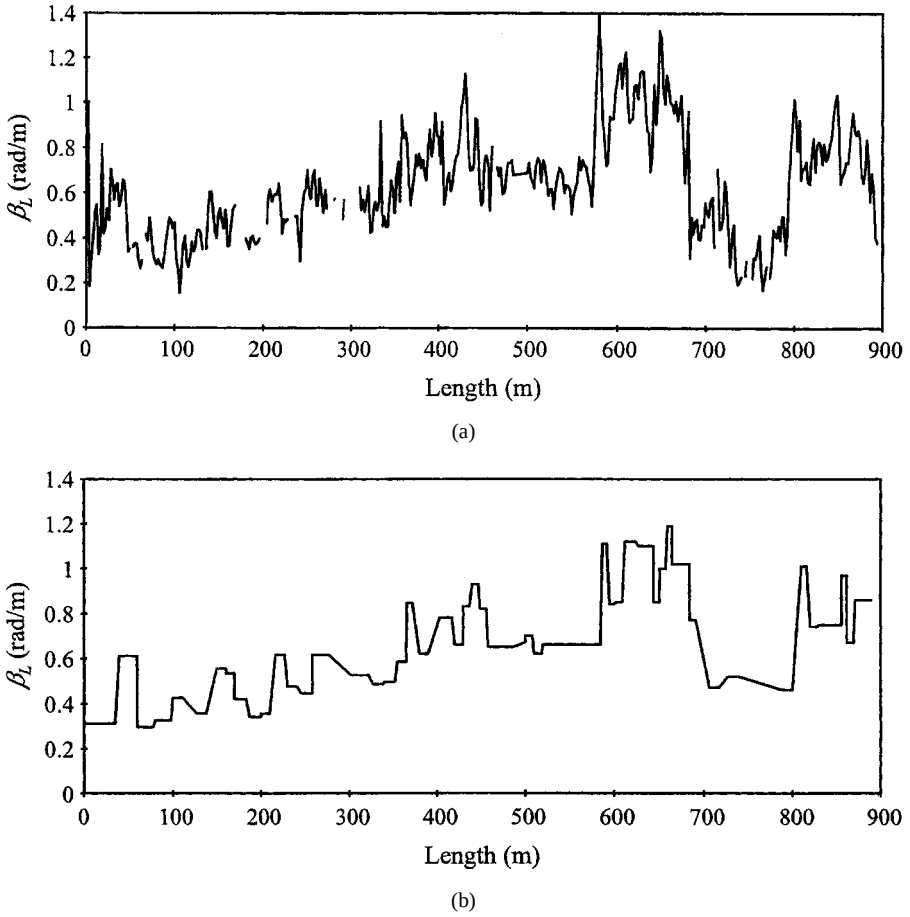

Fig. 6. Linear birefringence evolution along fiber 2 extracted using (a) the matrix method and (b) the best-fit method.

center of the bobbin (beyond ∼450 m). For instance, between 580 and 680 m the linear birefringence averages around 1 rad/m, while from 680 m to 800 m the linear birefringence is closer to 0.5 rad/m. This would suggest that near the beginning of the fiber spooling process, some systematic mechanism is inducing a tension variation in the fiber. This variation seems to settle down as more layers are wound onto the fiber, with the outermost layers in Fig. 6 showing an average linear birefringence value of around 0.4 rad/m.

For comparison, a section of fiber 2 was also analyzed off of the shipping bobbin, suspended in a 30 m catenary with the twist reduced to close to zero. Fig. 7 shows the corresponding backscattered SOP evolution, which when analyzed with the best-fit method gives a linear birefringence of 0.41 rad/m. This is comfortably close to the average linear birefringence obtained from the outermost layers of the fiber wound on the shipping bobbin.

To summarize, the linear birefringence behavior of fiber on a bobbin can be categorized into two regimes. Under high winding tension and/or for small diameter bobbins, the resulting bending birefringence dominates with the internal linear birefringence alternately adding and subtracting from this value. This behavior is illustrated by the section from 580 to 680 m in fiber 2. For low winding tension and/or large bobbins, the bending birefringence acts to modulate the value of the internal linear birefringence, as demonstrated by the behavior over the first 200 m of fiber 2.

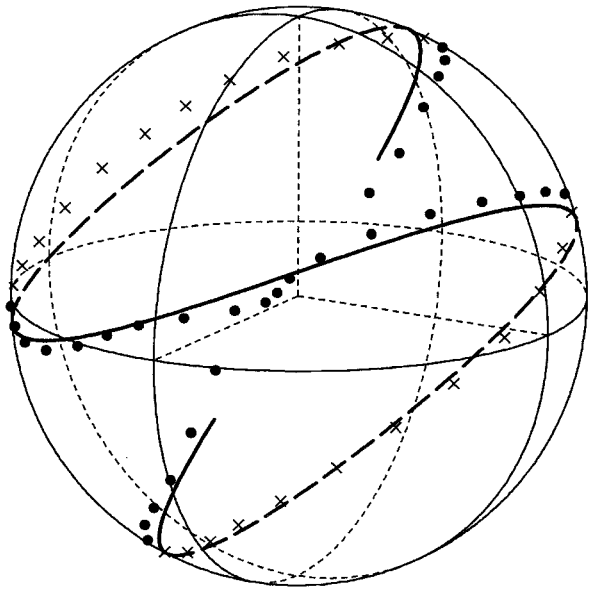

Fig. 7. Measured (points) and best-fit (solid line) backscattered SOP evolution for a 13-m section of fiber 2 suspended in a catenary giving $\beta_L = 0.41$ rad/m and $\tau = 0.08$ rad/m.

V. Conclusion

For POTDR to become a practicable, routine measurement tool, translation of the backscattered SOP data into the key fiber

parameters must be fully automatic and operator independent. In this paper, we have demonstrated a matrix-based analysis technique which can spatially resolve the linear birefringence and twist rate of the fiber under test without operator interaction. These key parameters allow the local DGD to be determined, from which the end-to-end PMD may be computed by integration [8]. The technique only requires the relative backscattered SOP to be measured, which considerably simplifies the POTDR design, and is immune to error propagation.

REFERENCES

[1] J. G. Ellison and A. S. Siddiqui, "A fully polarimetric optical time domain reflectometer," *IEEE Photon. Technol. Lett.*, vol. 10, pp. 246–248, Feb. 1998.

[2] R. E. Schuh and A. S. Siddiqui, "Single channel polarimetric OTDR for measurement of backscattered SOP evolution along a fiber with twist," *Electron. Lett.*, vol. 33, no. 25, pp. 2153–2154, 1997.

[3] A. J. Rogers, "Polarization-optical time domain reflectometry: A technique for the measurement of field distributions," *Appl. Opt.*, vol. 20, no. 6, pp. 1060–1074, 1981.

[4] J. N. Ross, "Birefringence measurement in optical fibers by polarization optical time-domain reflectometry," *Appl. Opt.*, vol. 21, no. 19, pp. 3489–3495, 1982.

[5] R. E. Schuh, J. G. Ellison, A. S. Siddiqui, and D. H. O. Bebbington, "Polarization OTDR measurements and theoretical analysis on fibers with twist and their implications for estimation of PMD," *Electron. Lett.*, vol. 32, no. 4, pp. 387–388, 1996.

[6] G. J. Foschini and C. D. Poole, "Statistical theory of polarization dispersion in single mode fibers," *J. Lightwave Technol.*, vol. 9, pp. 1439–1456, Nov. 1991.

[7] A. J. Rogers, Y. R. Zhou, and V. A. Handerek, "Computational polarization-optical time domain reflectometry for measurement of the spatial distribution of PMD in optical fibers," in *Proc. Conf. Dig. OFMC '97*, pp. 126–129.

[8] J. G. Ellison, "A polarimetric optical time domain reflectometer," Ph.D. dissertation, University of Essex, U.K., 1998.

J. G. Ellison, photograph and biography not available at the time of publication.

A. S. Siddiqui, photograph and biography not available at the time of publication.